Exploration of the effect and mechanism of *Eclipta prostrata L.* against gastric cancer based on network pharmacology and experimental verification

WEIZHOU YU[1*], XIAOHUI NI[2*], JING WANG[3], WEI XIA[3], XINYA SHEN[3], FAN QIU[4] and YUPING CHEN[3]

[1]Department of Gastroenterology, Dafeng People's Hospital of Yancheng City, Yancheng, Jiangsu 224100, P.R. China;
[2]Department of Orthopaedics, Dafeng People's Hospital of Yancheng City, Yancheng, Jiangsu 224100, P.R. China;
[3]Science and Technology Division, Jiangsu Medical College, Yancheng, Jiangsu 224005, P.R. China;
[4]School of Traditional Chinese Medicine, Jiangsu Medical College, Yancheng, Jiangsu 224005, P.R. China

Received December 17, 2025; Accepted March 27, 2026

DOI: 10.3892/ol.2026.15620

Abstract. The present study aimed to explore the therapeutic effects and underlying mechanisms of the active constituents of *Eclipta prostrata L.* in gastric cancer (GC) and to identify potential targets for its prevention and treatment. Active compounds and their corresponding targets were screened using the Traditional Chinese Medicine Systems Pharmacology Database and Analysis Platform. In comparison, GC-related targets were retrieved from GeneCards and Online Mendelian Inheritance in Man databases. Common targets were identified using Venny 2.1.0. Cytoscape 3.10.2 was then employed to construct a traditional Chinese medicine component-target-disease network and a protein-protein interaction network. Core compounds and targets were further assessed through molecular docking, and the potential mechanisms were investigated using Gene Ontology and Kyoto Encyclopedia of Genes and Genomes enrichment analyses. The biological activity of luteolin, the principal active component of *Eclipta prostrata L.*, was experimentally validated in AGS cells using Cell Counting Kit-8 assays, wound-healing (scratch) assays, Transwell migration assays, flow cytometry and western blotting. A total of 10 active ingredients and 166 shared targets were identified. Among them, quercetin, luteolin and acacetin were identified as key bioactive constituents, whereas AKT serine/threonine kinase 1 (AKT1), TNF and hypoxia-inducible factor-1 (HIF-1A) were recognized as central targets. Molecular docking analysis revealed strong binding affinities between the core compounds and these targets. Enrichment analyses further indicated that the therapeutic effects of *Eclipta prostrata L.* may involve pathways related to oxidative stress, the phosphatidylinositol 3-kinase-protein kinase B signaling pathway, and the HIF-1 signaling pathway. Among the identified compounds, luteolin showed the most pronounced inhibitory effects on GC cells and was therefore selected for further mechanistic investigation. *In vitro* experiments demonstrated that luteolin significantly suppressed GC cell proliferation and migration, reduced AKT phosphorylation and HIF-1A expression, and did not induce apoptosis. These findings suggest that luteolin may exert its anti-GC effects primarily by modulating the AKT1/HIF-1A signaling axis. The present study provides experimental support for the therapeutic potential of *Eclipta prostrata L.*-derived compounds and offers insights into novel molecular targets for GC treatment.

Correspondence to: Professor Yuping Chen, Science and Technology Division, Jiangsu Medical College, 283 South Jiefang Road, Yancheng, Jiangsu 224005, P.R. China
E-mail: 12064@jsmc.edu.cn

*Contributed equally

Abbreviations: AKT1, AKT serine/threonine kinase 1; BP, biological process; CC, cellular component; DL, drug likeness; EGFR, epidermal growth factor receptor; GC, gastric cancer; MF, molecular function; OB, oral bioavailability; PPI, protein-protein interaction; TCM, Traditional Chinese medicine; TNF, tumor necrosis factor; TP53, tumor protein p53; PI3K-Akt, phosphatidylinositol 3-kinase-protein kinase B; HIF-1, hypoxia-inducible factor-1

Key words: Eclipta prostrata L., luteolin, network pharmacology, GC, AKT, HIF-1A

Introduction

Gastric cancer (GC) remains one of the most common and deadly malignancies worldwide, posing a significant challenge to global public health. Although existing therapeutic approaches, including surgical resection, chemotherapy, radiotherapy and targeted therapy, have improved patient survival to some degree, several major challenges continue to limit their effectiveness, including high rates of recurrence and metastasis and treatment-associated adverse effects (1).

One major factor underlying these limitations is the significant heterogeneity of GC. Tumors arising in different patients frequently harbor diverse genetic alterations and molecular subtypes, leading to substantial variability in therapeutic responses and clinical outcomes (2). Conventional treatment

approaches are often accompanied by considerable toxicities. For example, chemotherapeutic agents frequently cause adverse effects such as nausea, vomiting and myelosuppression, which may limit their clinical application and adversely affect patients' quality of life (3). Therefore, identifying novel therapeutic targets and developing more effective and safer treatment strategies have become key priorities in GC research (4).

To this end, clarifying the molecular pathogenesis and core molecular drivers of GC is essential for identifying new therapeutic breakthroughs. The occurrence and development of GC is a complex multi-step process, mainly involving the abnormal activation of key signaling pathways including phosphatidylinositol 3-kinase (PI3K)-protein kinase B (Akt), hypoxia-inducible factor-1 (HIF-1) and tumor necrosis factor (TNF), as well as mutations of critical genes such as tumor protein p53 (TP53) and AKT serine/threonine kinase 1 (AKT1) (5,6). Core molecular drivers include the activation of oncogenes, such as epidermal growth factor receptor (EGFR) (7), the inactivation of tumor suppressor genes, such as TP53 (6), the abnormal activation of key signaling pathways, and the regulatory effects of epigenetic modifications and non-coding RNAs (8). However, the complex interactions among these drivers remain unclear, hindering the development of effective targeted therapies.

Traditional Chinese medicine (TCM) offers several advantages in the management of GC. Owing to its multi-component, multi-target and multi-pathway characteristics, TCM formulations can exert antitumor effects while also alleviating common clinical symptoms, including loss of appetite, nausea, vomiting and pain, improving patients' overall quality of life (9). Certain TCM-based therapies that focus on strengthening the body and restoring systemic balance may help enhance immune function and improve patients' tolerance to both the disease and subsequent therapeutic interventions (10). For example, curcumin from the TCM herb *Curcuma longa L.* exerts anti-GC effects by downregulating and blocking the Gli1/β-catenin pathway, suppressing GC cell proliferation and migration (11). The classic TCM formula Sijunzi Decoction modulates and acts against GC by regulating N6-methyladenosine modification to inhibit epithelial-mesenchymal transition (EMT) (12).

Eclipta prostrata L. is the dried aerial part of a plant belonging to the Asteraceae family. In TCM, it is described as having a sweet taste and a cold nature and is believed to act on the liver and kidney meridians. Clinically, it is commonly used to nourish the liver and kidneys, cool the blood, and promote hemostasis. Phytochemical studies have revealed that *Eclipta prostrata L.* contains a wide variety of bioactive constituents, including triterpenoid saponins, flavonoids, thiophenes and coumarin ethers. Modern pharmacological research has demonstrated that this plant possesses multiple biological activities, such as hemostatic, hepatoprotective, immunomodulatory, antitumor, anti-inflammatory, lipid-lowering, anti-hypoxic and anti-snake venom effects (13).

Despite these reported pharmacological activities, the specific bioactive constituents and molecular mechanisms by which *Eclipta prostrata L.* exerts therapeutic effects against GC remain incompletely understood, and systematic experimental validation remains limited. Therefore, the present study combines network pharmacology with experimental verification to identify the active components of *Eclipta prostrata L.* and clarify their potential mechanisms of action in the treatment of GC, providing a theoretical basis for its clinical application.

Materials and methods

Reagents and antibodies. The GC AGS cell line and gastric epithelial GES-1 cells were kindly donated by Dr Zhu Anqing (Jiangsu Medical College). Fetal bovine serum (FBS; cat. no. AB-FBS-1050S) was purchased from ShangHai ABW Company. RPMI-1640 medium (cat. no. 22400089), DMEM (cat. no. 11960-044) and trypsin-EDTA (0.25%; cat. no. 25200-056) were obtained from Gibco; Thermo Fisher Scientific, Inc. Luteolin (cat. no. HY-N0162; purity 99.51%) was obtained from ShangHai MedChemExpress.

The Cell Counting Kit-8 (CCK-8; cat. no. C0038), Annexin V-FITC cell apoptosis detection kit (cat. no. C1062M) and BeyoAOF™ serum-free cell cryopreservation solution (cat. no. C0210B) were purchased from Beyotime Institute of Biotechnology. Antibodies against HIF-1A (cat. no. sc-13515) were obtained from Santa Cruz Biotechnology, Inc., while antibodies against protein kinase B (AKT; cat. no. 4961) and phosphorylated AKT (p-AKT, Ser473; cat. no. 4060) were purchased from Cell Signaling Technology, Inc. β-actin (cat. no. 20536-1-AP) was purchased from Wuhan Sanying Biotechnology. The secondary antibodies were purchased from Boster Biological Technology, including goat anti-rabbit IgG (cat. no. BA1054) and goat anti-mouse IgG (cat. no. BA1050).

Screening of active components and target proteins of Eclipta prostrata L. The active ingredients of *Eclipta prostrata* L. were identified using the Traditional Chinese Medicine Systems Pharmacology Database and Analysis Platform (TCMSP; https://www.tcmsp-e.com/), with screening criteria set at oral bioavailability (OB) ≥30% and drug-likeness (DL) ≥0.18. The SMILES structures of the selected compounds were subsequently obtained from PubChem (https://pubchem.ncbi.nlm.nih.gov/).

These SMILES identifiers were then submitted to the SwissTargetPrediction platform (with species limited to humans; https://swisstargetprediction.ch/) to predict potential target genes associated with the active components of *Eclipta prostrata L.* Target gene names and related information were extracted based on the corresponding SMILES data. The predicted targets were further filtered using a probability threshold of ≥0.7. After removing duplicate entries, a total of 290 valid target genes associated with *Eclipta prostrata L.* were obtained.

Acquisition and screening of GC-related targets. Targets associated with GC were retrieved from the widely used disease-related databases GeneCards (https://www.genecards.org) and Online Mendelian Inheritance in Man (http://www.omim.org) using 'GC' as the search key word. The gene datasets obtained from these two databases were subsequently combined, and duplicate entries were removed to generate a unified list of GC-related genes.

To minimize potential interference from unvalidated targets and to improve the reliability of the subsequent analyses, the initial gene set was further refined by retaining only well-established GC driver genes that have been experimentally validated and reported in authoritative studies (1,4). These included core oncogenes, tumor suppressor genes, and key regulators involved in GC-specific signaling pathways.

Construction of TCM component-target-disease network and protein-protein interaction (PPI) network. The intersection between drug-related targets and disease-associated genes identified through the aforementioned approaches was determined using Venny (Venny 2.1.0; https://bioinfogp.cnb.csic.es/tools/venny/index.html), which generated both a Venn diagram and a list of overlapping genes. The active components, corresponding drug targets, and GC-related targets were then imported into Cytoscape (version 3.10.2; https://cytoscape.org/) for visualization and network analysis. Based on these datasets, a traditional Chinese medicine active component-target-disease interaction network was constructed to illustrate the potential therapeutic mechanisms of *Eclipta prostrata L*. in the treatment of GC.

The common targets shared between the drug and the disease were then uploaded to the STRING database (https://string-db.org) to construct a PPI network. The species parameter was limited to *Homo sapiens*, and the interaction confidence score was set to the highest confidence level (>0.900), while all other parameters were maintained at their default settings. The resulting protein interaction data were downloaded in TSV format and imported into Cytoscape 3.10.2 for visualization. Proteins that did not interact with any other nodes in the network were excluded from the analysis.

Network topology was further analyzed using the Network Analyzer tool within Cytoscape. The Degree value, defined as the number of direct connection edges linked to a given node, was calculated for each target. This metric reflects the extent of interaction between a node and other nodes in the network, with higher Degree values indicating greater biological importance. Using the 'Analyze Network' function in the 'Tools' menu, degree values were calculated for all nodes, and a corresponding PPI network diagram was generated. Based on these topological parameters, key targets closely associated with GC were subsequently identified.

Gene Ontology (GO) analysis and Kyoto Encyclopedia of Genes and Genomes (KEGG) enrichment pathway analysis. The shared targets between the drug and the disease identified in the aforementioned analyses were uploaded to the Metascape platform (http://metascape.org/gp/index.html), with the species parameter set to *Homo sapiens*. The 'Custom Analysis' option was selected, and the significance threshold for both GO analysis and KEGG pathway enrichment analysis was set at $P<0.01$.

The GO enrichment analysis included three functional categories: Biological processes (BP), cellular components (CC) and molecular functions (MF). All relevant results were exported and saved for subsequent interpretation. The enrichment outcomes from the GO and KEGG analyses were then visualized using a bioinformatics visualization tool (https://www.bioinformatics.com.cn/), which generated column and bubble charts to illustrate the distribution and significance of the enriched terms and pathways.

Molecular docking verification of active components and key targets of the drug. Molecular docking was conducted to simulate intermolecular interactions between ligands and receptors, enabling the prediction of potential binding modes and affinities between candidate drug molecules and the three-dimensional structures of target proteins. This method enabled the identification of key active compounds and their potential therapeutic targets. Based on the Degree values of drug components in the drug-target-disease network and those of nodes in the PPI network, representative active ingredients and core target proteins were selected for molecular docking validation.

The molecular structures of the active ingredients were obtained from the TCMSP database, while the three-dimensional structures of the corresponding target proteins were retrieved from the Protein Data Bank (RCSB; http://www.rcsb.org/). Before docking, the molecular structures were prepared using PyMOL (version 3.1.8; https://pymol.org/), including the addition of hydrogen atoms and removal of water molecules. Molecular docking between the selected compounds and target proteins was then performed using AutoDock Vina (version 1.1.2; https://vina.scripps.edu/). Finally, the docking conformations and interaction results were visualized and analyzed using PyMOL.

Culture of GC AGS and gastric epithelial GES-1 cell line. AGS cells were cultured in RPMI-1640 medium supplemented with 10% FBS and maintained in a humidified incubator at 37˚C with 5% CO_2. The culture medium was replaced every two days, and the cells were passaged using 0.25% trypsin for enzymatic digestion. The gastric epithelial cell line GES-1 was cultured in DMEM supplemented with 10% FBS. When the cell confluence reached 80-90%, the cells were digested with 0.25% trypsin-EDTA for subculture. Cells in the logarithmic growth phase were used for all experiments.

CCK-8 assay. AGS cells in the logarithmic growth phase were digested and resuspended to prepare a single-cell suspension, which was then seeded into 96-well plates at a density of 5,000 cells per well. A blank control group, a DMSO control group, and treatment groups with different drug concentrations were established, with six replicate wells for each condition. Based on the network pharmacology analysis, the representative active compounds quercetin, acacetin and luteolin were selected for further investigation.

After overnight incubation to allow cell adhesion, the treatment groups were exposed to different concentrations of the selected compounds (5, 12.5, 25, and 50 μM) for 24 and 48 h. CCK-8 reagent (20 μl) was then added to each well, and the cells were incubated for another 1 h at 37˚C. Cell viability was then determined by measuring the absorbance at 450 nm using a microplate reader. To determine the sub-toxic concentrations of luteolin that do not affect cell proliferation, concentrations that exerted no significant inhibitory effect (inhibition rate <5%) were defined as sub-toxic. Accordingly, 5 and 12.5 μM luteolin were selected as sub-toxic concentrations for wound healing and Transwell migration assays to avoid interference

from cell proliferation. The CCK-8 assay was used to assess the viability of normal gastric epithelial GES-1 cells after 48 h of incubation. Luteolin showed no significant cytotoxicity in GES-1 cells at 5, 12.5, 25 and 50 μM (inhibition rate <5%), indicating that these concentrations are safe.

Detection of cell migration rate by cell scratch test and migration test

Scratch assay. AGS cells in logarithmic growth phase were digested to obtain a single-cell suspension, then seeded into 6-well plates. The cells were divided into a blank control group, a DMSO control group, and luteolin treatment groups (5 and 12.5 μM). After reaching full confluence, cells were serum-starved in RPMI-1640 medium (cat. no. 22400089; Gibco; Thermo Fisher Scientific, Inc.) for 12 h to minimize proliferation interference. During the subsequent scratch assay, cells were maintained in serum-free RPMI-1640 medium corresponding to each treatment group. A linear scratch was then made across the cell monolayer using a sterile 20-μl pipette tip. Following washing with PBS to remove detached cells, the corresponding treatments were added, and the plates were incubated at 37˚C. Wound closure was observed under an inverted light microscope at 24 and 48 h, and the cell migration rate was calculated using the formula: Migration rate=(scratch area at 0 h-scratch area at 24 or 48 h)/scratch area at 0 h.

Transwell migration assay. AGS cells in the logarithmic growth phase were adjusted to a density of $2x10^5$ cells/ml and suspended in serum-free RPMI-1640 medium, and then seeded into the upper chambers of Transwell inserts with 8-μm pores. Luteolin (5 and 12.5 μM) or an equal volume of DMSO was added to the upper chamber medium, while the lower chambers were filled with RPMI-1640 medium supplemented with 10% FBS. The chambers were placed in 24-well plates and cells were incubated at 37˚C for 24 h. After incubation, the chambers were removed, and the non-migratory cells on the upper surface of the membrane were carefully removed using a cotton swab. The migratory cells were subsequently fixed with 4% paraformaldehyde at 37˚C for 15 min and stained with 0.1% crystal violet at room temperature for 30 min. Images were captured using an inverted fluorescence microscope (Olympus Corporation). A total of five random microscopic fields were then selected for imaging and quantitative assessment of the migratory cells.

Detection of AGS cell apoptosis by flow cytometry. AGS cells were collected and transferred to centrifuge tubes, then washed twice with PBS. A cell suspension containing $5x10^4$ cells was prepared and centrifuged at 1,000 x g for 5 min, after which the supernatant was carefully discarded. Subsequently, 195 μl of Annexin V-FITC binding buffer was added to resuspend the cell pellet gently.

Next, 5 μl of Annexin V-FITC reagent was added, followed by 10 μl of propidium iodide staining solution, with gentle mixing after each addition. The cells were incubated at room temperature in the dark for 10-20 min, then placed on ice. Finally, apoptosis was assessed by flow cytometry using a cyFlow Space Sorter (Sysmex Corporation), allowing quantification of early and late apoptotic cells and necrotic cells. The resulting data were recorded and analyzed using FlowJo software (version 10.8.1; FlowJo LLC).

Western blotting. AGS cells in the logarithmic growth phase were digested to obtain a single-cell suspension and then seeded into 6-well plates. The cells were divided into a DMSO control group and luteolin treatment groups (25 and 50 μM). Following treatment, the cells were washed twice with PBS, and total cellular proteins were extracted using RIPA lysis buffer (cat. no. R0010; Beijing Solarbio Science & Technology Co., Ltd.). Protein concentrations were measured using the BCA assay.

Protein loading buffer was subsequently added, and the samples were denatured at 95˚C for 5 min before electrophoresis. A total of 30 μg of protein was loaded per lane. Proteins were separated by 10% SDS-PAGE (cat. no. P1200; Beijing Solarbio Science & Technology Co., Ltd.) and transferred onto 0.45-μm PVDF membranes (cat. no. IPVH00010; MilliporeSigma). The membranes were then blocked with 5% skim milk for 2 h at 37˚C and incubated overnight at 4˚C with the corresponding primary antibodies at the following dilutions: AKT and p-AKT at 1:1,000, HIF-1A at 1:250, and β-actin at 1:5,000. On the following day, the membranes were washed with PBS containing 0.1% Tween-20 (cat. no. T8220; Beijing Solarbio Science & Technology Co., Ltd.) and incubated with HRP-conjugated secondary antibodies at a dilution of 1:5,000 at room temperature for 2 h. Protein bands were detected using enhanced chemiluminescence (ECL; cat. no. WBKLS0500; MilliporeSigma).

The grayscale intensity of each band was quantified using ImageJ (version 2.x; National Institutes of Health), with β-actin serving as the internal reference. Relative changes in the expression levels of the target proteins were then calculated.

Statistical analysis of data. All data are presented as the mean ± standard deviation (SD). The CCK-8 cell proliferation assay was performed in six independent replicates, while all other experiments were conducted in triplicate. Statistical analyses were conducted using SPSS (version 19.0; IBM Corp.). Differences among groups were assessed by one-way analysis of variance, followed by the LSD-t post hoc test for pairwise comparisons. $P<0.05$ was considered to indicate a statistically significant difference.

Results

Acquisition and screening of active components and drug-related targets of Eclipta prostrata L. The active ingredients of *Eclipta prostrata L*. were obtained from the TCMSP database. Applying the screening criteria of OB ≥30% and DL ≥0.18, a total of 10 active compounds were identified (Table I). The SMILES structures of these compounds were then used to predict potential target genes through the SwissTargetPrediction platform, with the species limited to humans. The predicted targets were subsequently filtered by probability, and duplicate entries were removed to generate the final set of targets associated with the drug's active components.

Acquisition of potential targets of Eclipta prostrata L. in intervening GC. Using 'GC' and 'gastric carcinoma' as search keywords, disease-related targets were retrieved from the GeneCards and Online Mendelian Inheritance in Man databases. After removing duplicate entries, a consolidated

Table I. Information on the active ingredients of *Eclipta prostrata L.*

Mol ID	Molecule name	Chemical formula	Molecular weight	Oral bioavailability (%)	Drug likeness	Content in *Eclipta prostrata L.* (%, dry weight)
MOL003404	Wedelolactone	$C_{16}H_{10}O_7$	314.26	49.6	0.48	0.045-0.062
MOL003402	Demethyl wedelolactone	$C_{17}H_8O_7$	302.25	72.13	0.43	0.032-0.041
MOL003398	Pratensein	$C_{16}H_{12}O_6$	299.27	39.06	0.28	0.015-0.020
MOL003389	3'-O-METHYLOROBOL	$C_{16}H_{12}O_6$	300.28	57.41	0.27	0.012-0.016
MOL003378	1,3,8,9-tetrahydroxybenzofurano [3,2-c]chromen-6-one	$C_{17}H_8O_7$	300.23	33.94	0.43	0.009-0.013
MOL002975	Butin	$C_{17}H_{12}O_7$	272.27	69.94	0.21	0.022-0.028
MOL001790	Linarin	$C_{28}H_{32}O_{14}$	592.6	39.84	0.71	0.010-0.015
MOL001689	Acacetin	$C_{16}H_{12}O_7$	284.28	34.97	0.24	0.008-0.011
MOL000098	Quercetin	$C_{17}H_{10}O_7$	302.25	46.43	0.28	0.015-0.018
MOL000006	Luteolin	$C_{17}H_{10}O_6$	286.25	36.16	0.25	0.021-0.035

list of GC-related target genes was obtained. The initial gene set was then further refined by retaining only well-established driver genes reported in authoritative GC studies (1,4), excluding unvalidated candidate genes and reducing potential analytical bias.

Subsequently, the intersection between the drug-related targets and disease-associated genes was identified using Venny (Venny 2.1.0). A total of 166 common targets shared between *Eclipta prostrata L.* and GC were obtained. The overlap of these targets is illustrated in a Venn diagram (Fig. 1).

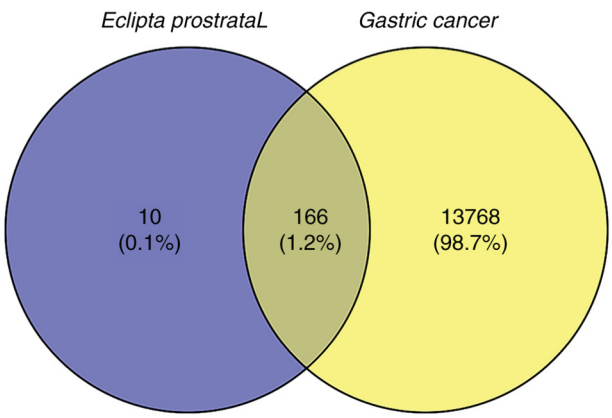

Figure 1. Venn diagram of the common targets between the active ingredients of *Eclipta prostrata L.* and gastric cancer.

TCM component-target-disease network. The identified active ingredients of *Eclipta prostrata L.* and their shared targets with GC were imported into Cytoscape (version 3.10.2) to construct the TCM component-target-disease interaction network. In the resulting network diagram, the purple polygon represents *Eclipta prostrata L.*, blue rectangles indicate its active components, green ellipses correspond to the 166 shared targets, and the orange node represents GC (Fig. 2A).

Topological analysis of the network was conducted using the Network Analyzer tool in Cytoscape. The Degree value represents the number of direct interactions between a component and its targets; thus, a higher Degree value indicates greater influence within the network. Based on this metric, the three compounds with the highest Degree values were quercetin, luteolin and acacetin. To delineate the core bioactive constituents underlying the anti-GC effects of *Eclipta prostrata L.*, simplified component-target-disease networks for the major active ingredients were constructed using Cytoscape 3.10.2. As summarized in Fig. 2B-D, network analysis revealed robust and intricate target connectivity profiles for quercetin, luteolin and acacetin. These data collectively validate that the three flavonoids are the principal active components of *Eclipta prostrata L.*, and that a sophisticated multi-target regulatory mechanism underpins their anti-GC activities.

Construction of the PPI network and analysis of core targets. The PPI network comprised 166 nodes. As shown in Fig. 3A, the size and color intensity of each node reflected its Degree value, with larger and darker nodes indicating a higher level of connectivity within the network. The top 10 target proteins, ranked by Degree, are presented in Table II.

MCODE clustering analysis identified three significant subnetworks, with scores of MCODE Cluster 1=54.866, MCODE Cluster 2=4.273 and MCODE Cluster 3=2.889 (Fig. 3B-D). Analysis of the PPI network indicated that several key targets, including AKT1, TNF, TP53, IL6, IL1B, CASP3, JUN, PTGS2, EGFR and HIF-1A, are closely associated with GC. These findings suggest that these proteins may play important roles in mediating the therapeutic effects of *Eclipta prostrata L.* in GC.

Results of molecular docking verification. The three compounds with the highest Degree values in the 'TCM component-target-disease network', quercetin, luteolin and acacetin, together with the 10 potential core targets demonstrating the highest Degree values, namely AKT1, TNF, TP53, IL6, IL1B, CASP3, JUN, PTGS2, EGFR and HIF-1A, were selected for molecular docking analysis.

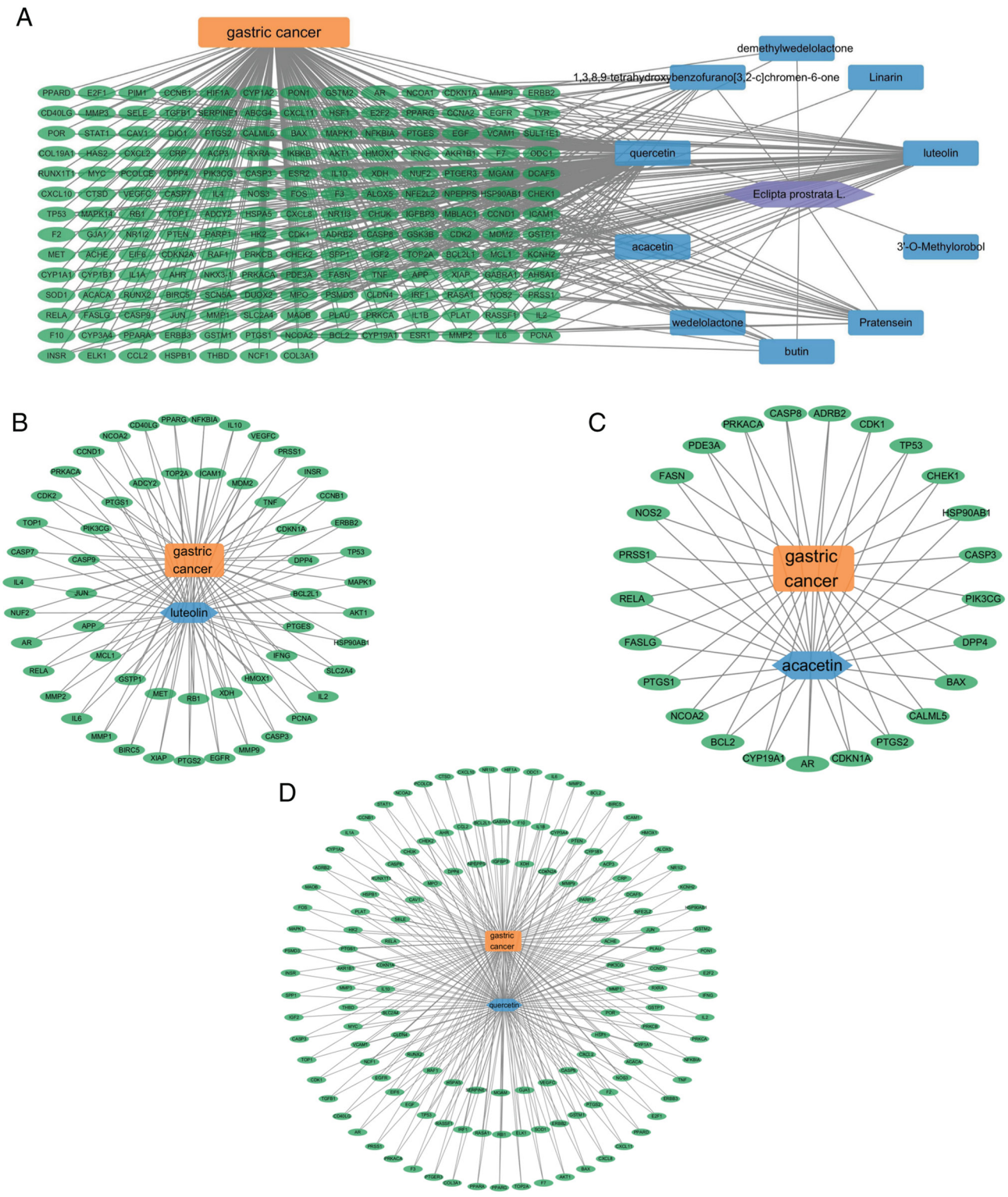

Figure 2. Component-target-disease interaction networks of major active ingredients from *Eclipta prostrata L.* in GC. (A) Global view of the integrated component-target-disease network. The orange diamond node represents GC; blue rectangles denote active ingredients from *Eclipta prostrata L.*; green ellipses indicate shared target genes; and the purple polygon node represents *Eclipta prostrata L.* (B-D) Simplified topological networks for core active ingredients: (B) Luteolin, (C) acacetin and (D) quercetin. GC, gastric cancer.

According to the binding energy criterion, where values <-5.0 kcal·mol^{-1} indicate favorable interactions, the docking results showed that quercetin, luteolin, and acacetin all displayed binding energies below this threshold (Table III), suggesting stable and favorable interactions with their predicted targets. Subsequent cellular experiments revealed that luteolin exerted a stronger inhibitory effect on AGS cell proliferation than quercetin or acacetin. To further clarify the molecular basis underlying this enhanced activity, the binding modes of luteolin with the 10 core targets were examined using both three-dimensional structural alignment and two-dimensional interaction analysis. As illustrated by the 3D

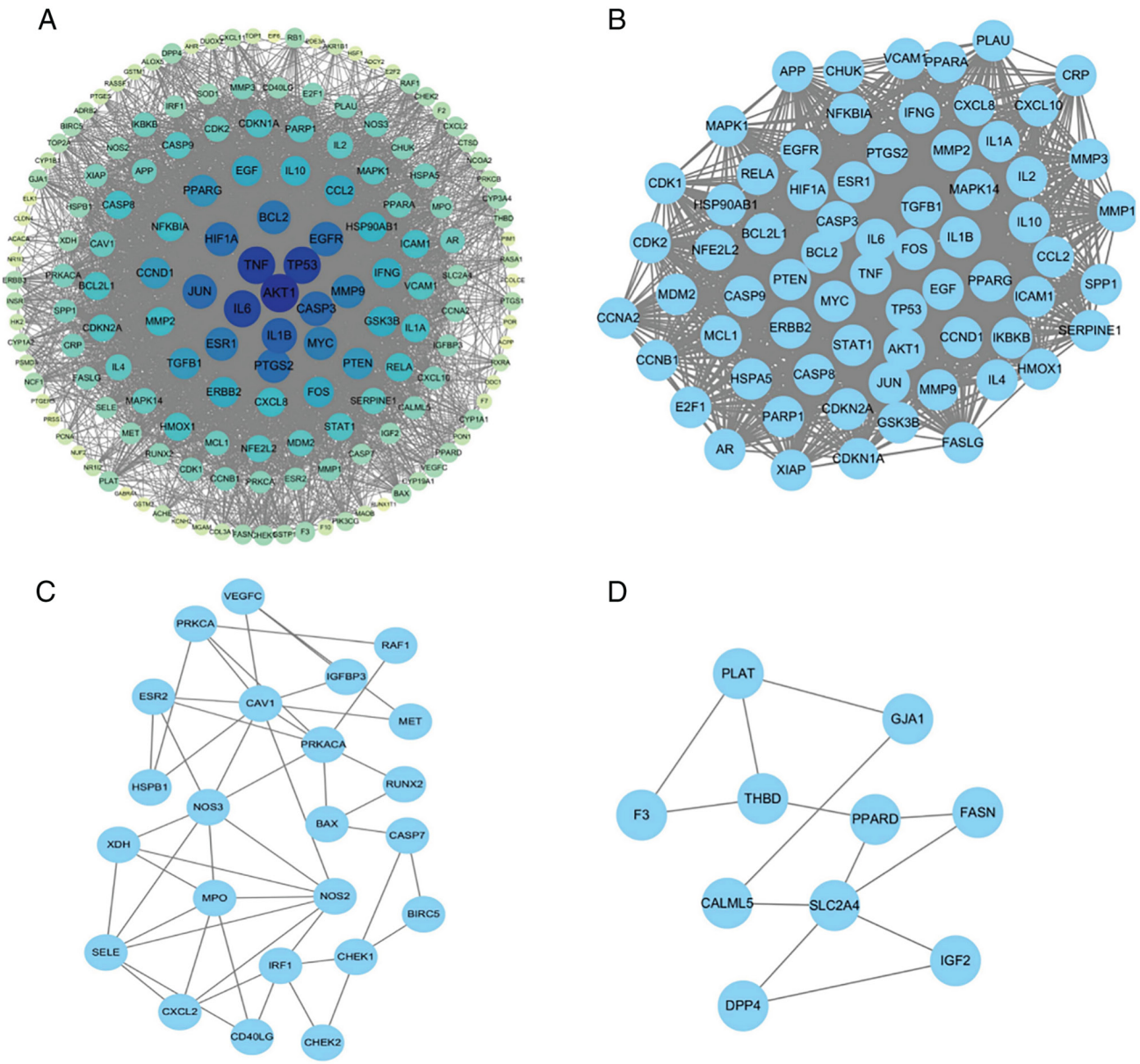

Figure 3. PPI network analysis and identification of core targets for *Eclipta prostrata L.* in the treatment of gastric cancer. (A) PPI network. (B) MCODE cluster 1. (C) MCODE cluster 2. (D) MCODE cluster 3. PPI, protein-protein interaction.

docking conformations (Fig. 4), luteolin successfully docked into the active sites of all 10 potential core targets, forming stable conformations stabilized by key molecular interactions. Furthermore, the high-resolution 2D interaction maps (Fig. S1) provided atomic-level insights, revealing that luteolin binding was primarily anchored by conventional hydrogen bonds and extensive hydrophobic interactions. Notably, luteolin specifically bound to critical functional domains of key GC-related targets, including the ATP-binding catalytic pocket of AKT1 and the transactivation domain of HIF-1A, essential structural regions required for their biological activities. These combined 3D and 2D analyses validate the robust binding capacity of luteolin and elucidate the specific molecular basis by which it modulates the functions of these core targets.

Results of GO and KEGG enrichment analyses. To further clarify the potential core targets and pathological mechanisms through which *Eclipta prostrata L.* exerts therapeutic effects against GC, GO and KEGG pathway enrichment analyses were performed on the shared targets identified between *Eclipta prostrata L.* and GC.

The GO enrichment analysis results (Fig. 5A) showed that the major BP associated with the therapeutic effects of *Eclipta prostrata L.* in GC included responses to lipopolysaccharide, bacterial-derived molecules, xenobiotic stimuli, cellular chemical stress and oxidative stress. The enriched CC were mainly associated with membrane rafts, membrane microdomains, protein kinase complexes, vesicle lumens and serine/threonine protein kinase complexes. Regarding MF, the identified targets were primarily involved in DNA-binding transcription factor binding, RNA polymerase II-specific DNA-binding transcription factor binding, cytokine receptor binding, ubiquitin-like protein ligase binding, and nuclear receptor activity (Fig. 5A).

Table II. Target proteins with the top 10 degree values in the protein-protein interaction network diagram.

Serial number	Target	Degree value
1	AKT1	130
2	TNF	126
3	TP53	125
4	IL6	123
5	IL1B	115
6	CASP3	112
7	JUN	111
8	PTGS2	110
9	EGFR	110
10	HIF1A	109

AKT1, AKT serine/threonine kinase 1; EGFR, epidermal growth factor receptor; TNF, tumor necrosis factor; TP53, tumor protein p53; HIF-1, hypoxia-inducible factor-1.

Table III. Molecular docking results of active ingredients of *Eclipta prostrata L.* and common targets.

	Affinity/(kcal·mol-1)		
Gene	Acacetin	Luteolin	Quercetin
TP53	-7.4	-7.5	-6.8
IL6	-7.7	-7.8	-7.7
PTGS2	-9.1	-9.2	-9.7
CASP3	-7.2	-7.1	-7
JUN	-8.1	-8.4	-8.5
TNF	-7	-6.8	-6.7
AKT1	-6.5	-6.4	-6.5
EGFR	-9.4	-9.3	-8.7
HIF1A	-6.9	-6.9	-6.5
IL1B	-7.2	-7.5	-6.9

AKT1, AKT serine/threonine kinase 1; EGFR, epidermal growth factor receptor; TNF, tumor necrosis factor; TP53, tumor protein p53; HIF-1, hypoxia-inducible factor-1.

KEGG pathway enrichment analysis further indicated that the potential mechanisms may involve several cancer-related signaling pathways, including the TNF signaling pathway, PI3K-Akt signaling pathway, p53 signaling pathway, MAPK signaling pathway and HIF-1 signaling pathway (Fig. 5B). These results suggest that multiple signaling networks may collectively contribute to the anti-GC effects of *Eclipta prostrata*.

Effect of luteolin, the main component of Eclipta prostrata L., on the proliferation and migration of GC AGS cell line. The CCK-8 assay was conducted to assess the effects of the three principal active compounds, luteolin, acacetin and quercetin, on the proliferation of AGS cells. The results indicated that quercetin (25 and 50 μM) did not significantly influence cell viability after either 24 or 48 h of treatment. Similarly, acacetin (25 and 50 μM) showed no significant effect on cell viability after 24 h of exposure; however, treatment with 50 μM acacetin for 48 h resulted in an excessively high inhibitory rate on cell proliferation (69.8%) (Fig. S2A and B).

In comparison, treatment with 50 μM luteolin for 24 h significantly suppressed AGS cell proliferation ($P<0.001$). After 48 h of exposure to 25 and 50 μM luteolin, the inhibitory rates in the treatment groups were significantly higher than those observed in the DMSO control group ($P<0.001$) (Fig. 6C).

Therefore, luteolin was selected for further investigation because it exhibited a more potent and moderate inhibitory effect on AGS cell proliferation compared with quercetin and acacetin. In addition, luteolin is a well-known flavonoid with established safety and potent antitumor activity in various cancer models, supporting its rationality as the key component for mechanistic research (14,15).

To identify sub-toxic concentrations of luteolin that would not affect cell proliferation, an additional CCK-8 assay was performed. Concentrations producing no significant inhibitory effect on cell viability (inhibition rate <5%) were defined as sub-toxic. Based on this analysis, 5 and 12.5 μM luteolin were selected for subsequent wound healing and Transwell migration assays to ensure that any observed changes in migration were independent of effects on cell proliferation (Fig. 6C). The wound healing (scratch) assay demonstrated that after 48 h of incubation, the migration rate of cells treated with luteolin (12.5 μM) was significantly reduced compared with that of the DMSO control group ($P<0.05$) (Fig. 6A and D).

To further evaluate cell migration, a Transwell assay using 8-μm pore chambers was performed at 24 and 48 h of culture. In the DMSO group, a large number of crystal violet-stained cells were observed on the lower surface of the membrane, indicating substantial migratory activity. In comparison, the number of migratory cells in the luteolin-treated group (12.5 μM) was significantly reduced compared with the control group, showing a statistically significant difference ($P<0.01$) (Fig. 6B and E).

Cytotoxicity of luteolin on normal gastric epithelial GES-1 cells. To ensure the safety of the working concentrations used in migration assays, the cytotoxicity of luteolin on normal gastric epithelial GES-1 cells was detected by CCK-8 assay. As shown in Fig. S2C, treatment with 5, 12.5, 25, or 50 μM luteolin for 48 h showed no significant effect on GES-1 cell viability, with inhibition rates <5%. These results clearly indicated that luteolin exerted no obvious toxic effect on normal gastric mucosal epithelial cells at the concentrations used for subsequent migration experiments (Fig. S2C).

Effect of luteolin, the main component of Eclipta prostrata L., on the apoptosis of GC cell line. Flow cytometry was performed to determine the combined proportion of early- and late-apoptotic AGS cells after treatment with luteolin (25 and 50 μM) for 48 h. The results showed that the average apoptotic rate in the DMSO control group was 17.7%, whereas the rates in the 25 and 50 μM luteolin treatment groups were 16.7 and 18.02%, respectively. No statistically significant differences were detected among the three groups (Fig. 7).

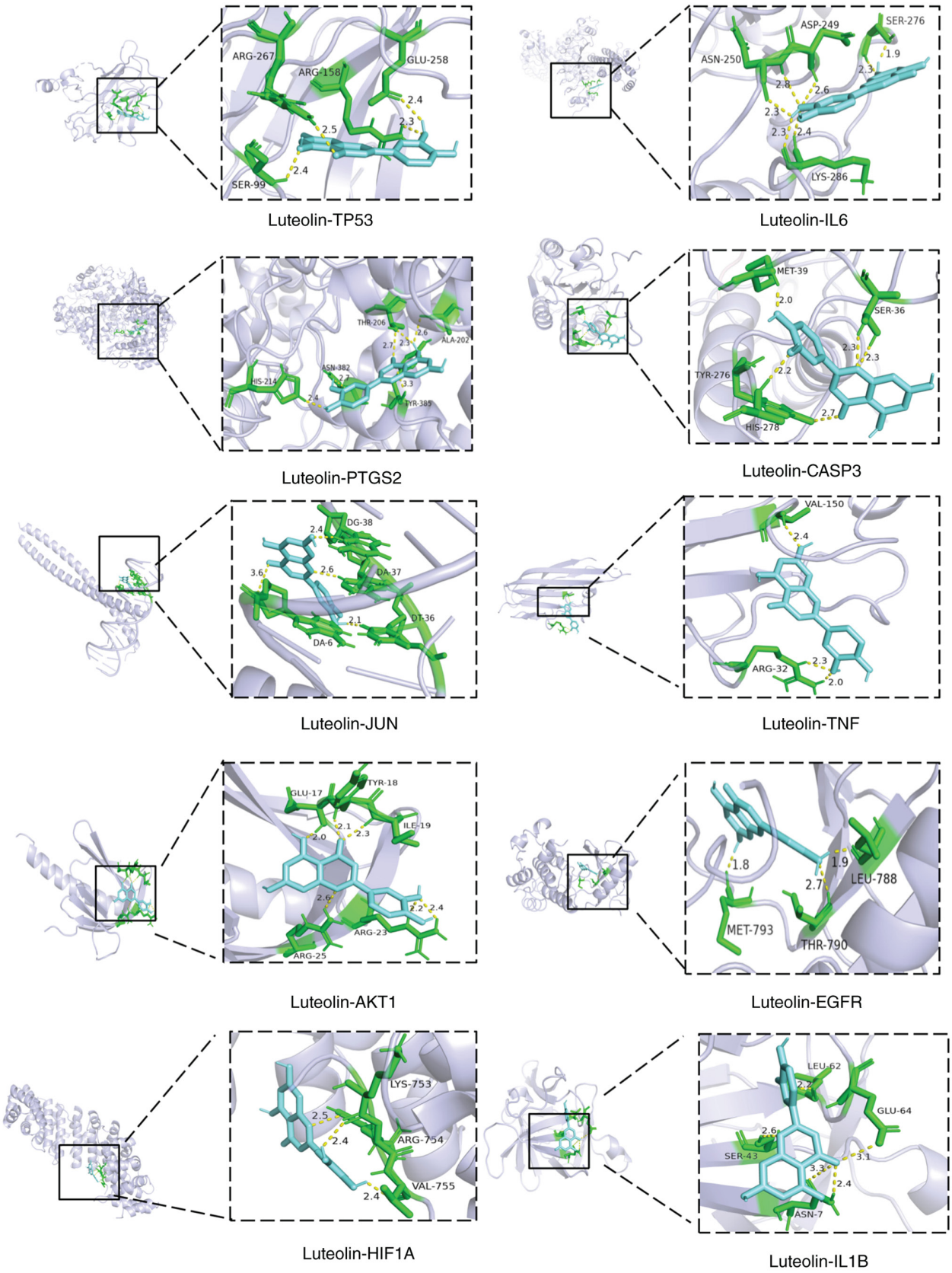

Figure 4. Molecular docking result diagram of luteolin and core targets. AKT1, AKT serine/threonine kinase 1; EGFR, epidermal growth factor receptor; TNF, tumor necrosis factor; TP53, tumor protein p53; HIF-1, hypoxia-inducible factor-1.

Effect of luteolin, the main component of Eclipta prostrata L., on the core targets AKT and HIF-1A of GC cell line. GO and KEGG enrichment analyses revealed that the serine/threonine protein kinase complex and the HIF-1 signaling pathway were among the major pathways associated with the shared targets of *Eclipta prostrata L.* and GC. To further explore this

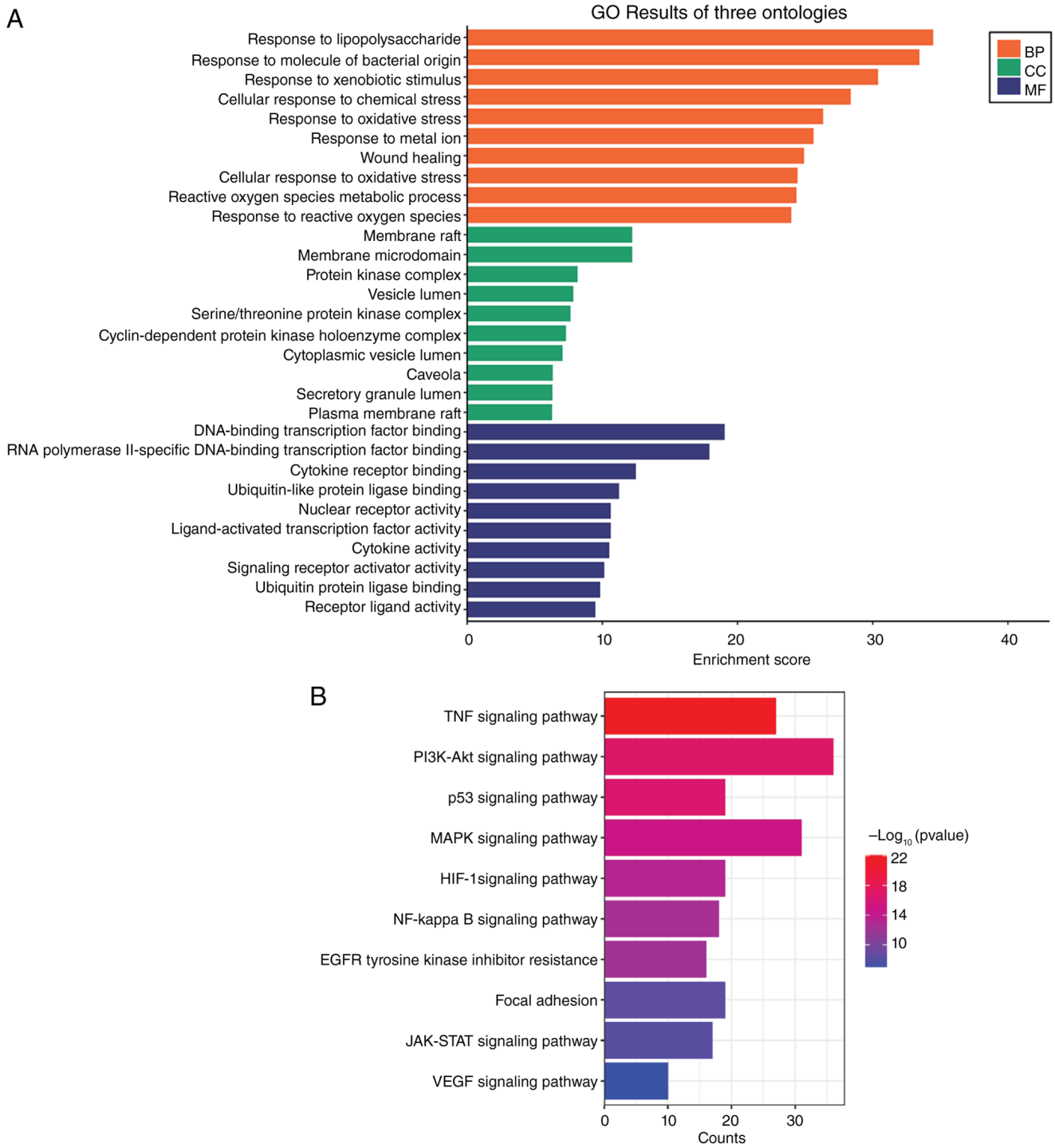

Figure 5. GO and KEGG enrichment analyses of the common targets. (A) GO enrichment analysis. (B) KEGG enrichment analysis. GO, Gene Ontology; KEGG, Kyoto Encyclopedia of Genes and Genomes; BP, biological process; MF, molecular function; CC, cellular component.

mechanism, western blot analysis was conducted to evaluate the effects of luteolin on the expression of the core target proteins AKT1 and HIF-1A in GC cells.

The results showed that, compared with the DMSO control group, treatment with 25 or 50 μM luteolin significantly reduced AKT phosphorylation at Ser473, and it decreased the protein expression level of HIF-1A in GC cells (Fig. 8A-D). These findings suggest that luteolin may inhibit the proliferation and migration of GC cells by modulating the key regulatory proteins AKT1 and HIF-1A.

Discussion

GC remains the fifth most frequently diagnosed malignancy and the fourth leading cause of cancer-related death worldwide. Despite ongoing advances in therapeutic strategies, several significant limitations remain. Conventional treatments, including surgery, chemotherapy and radiotherapy, can effectively eliminate tumor cells; however, their clinical effectiveness is often limited by chemotherapy resistance, considerable toxicity and adverse effects, high rates of

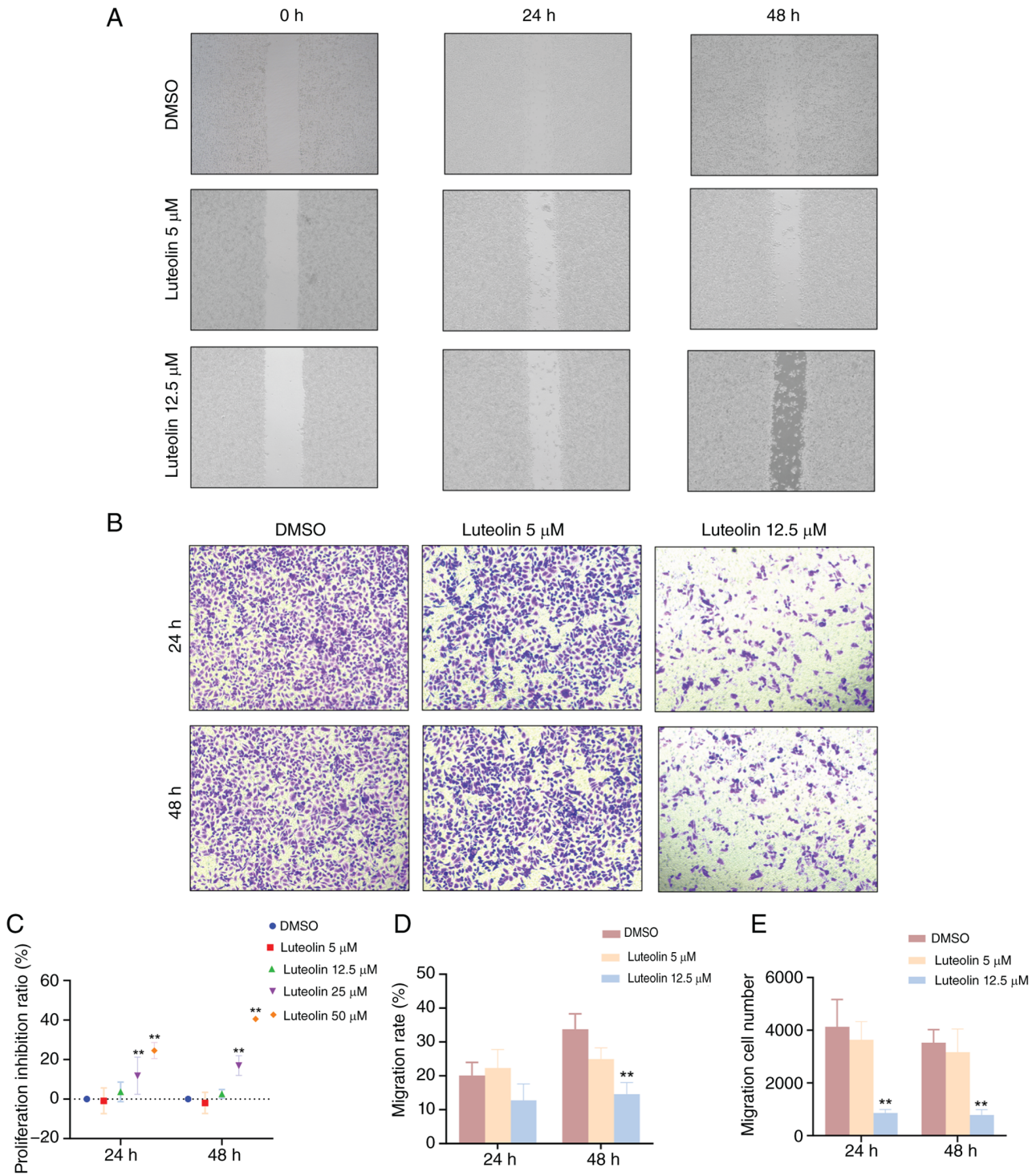

Figure 6. Effects of luteolin on the proliferation and migration of gastric cancer AGS cell line. (A and D) Detection of the migration rate by the cell scratch assay, cells were treated with luteolin (12.5, 25 μM) for 24 or 48 h. Values are expressed as the mean ± SD (n=3). (B and E) Detection of the cell migration ability by the Transwell assay, cells were treated with luteolin (12.5, 25 μM) for 24 or 48 h. Values are expressed as the mean ± SD (n=3). (C) Detection of the cell proliferation activity by the Cell Counting Kit-8 assay, cells were treated with luteolin (0, 5, 12.5, 25, 50 μM) for 24 or 48 h. Values are expressed as the mean ± SD (n=6). Compared with DMSO control, **P<0.01.

postoperative recurrence and treatment-related immunosuppression (1). In comparison, TCM provides a complementary therapeutic approach characterized by multi-component and multi-target synergistic effects. Through these mechanisms, TCM has shown potential to inhibit tumor cell proliferation, promote apoptosis, suppress angiogenesis, and regulate the tumor immune microenvironment (9).

Eclipta prostrata L., a traditional herbal medicine known for its yin-nourishing and blood-cooling properties, has attracted increasing attention for its potential antitumor activity. Phytochemical investigations have revealed that its major bioactive constituents include alkaloids, flavonoids and polysaccharides (13). Previous studies have shown that ethanol extracts of *Eclipta prostrata L.* can exert anticancer effects

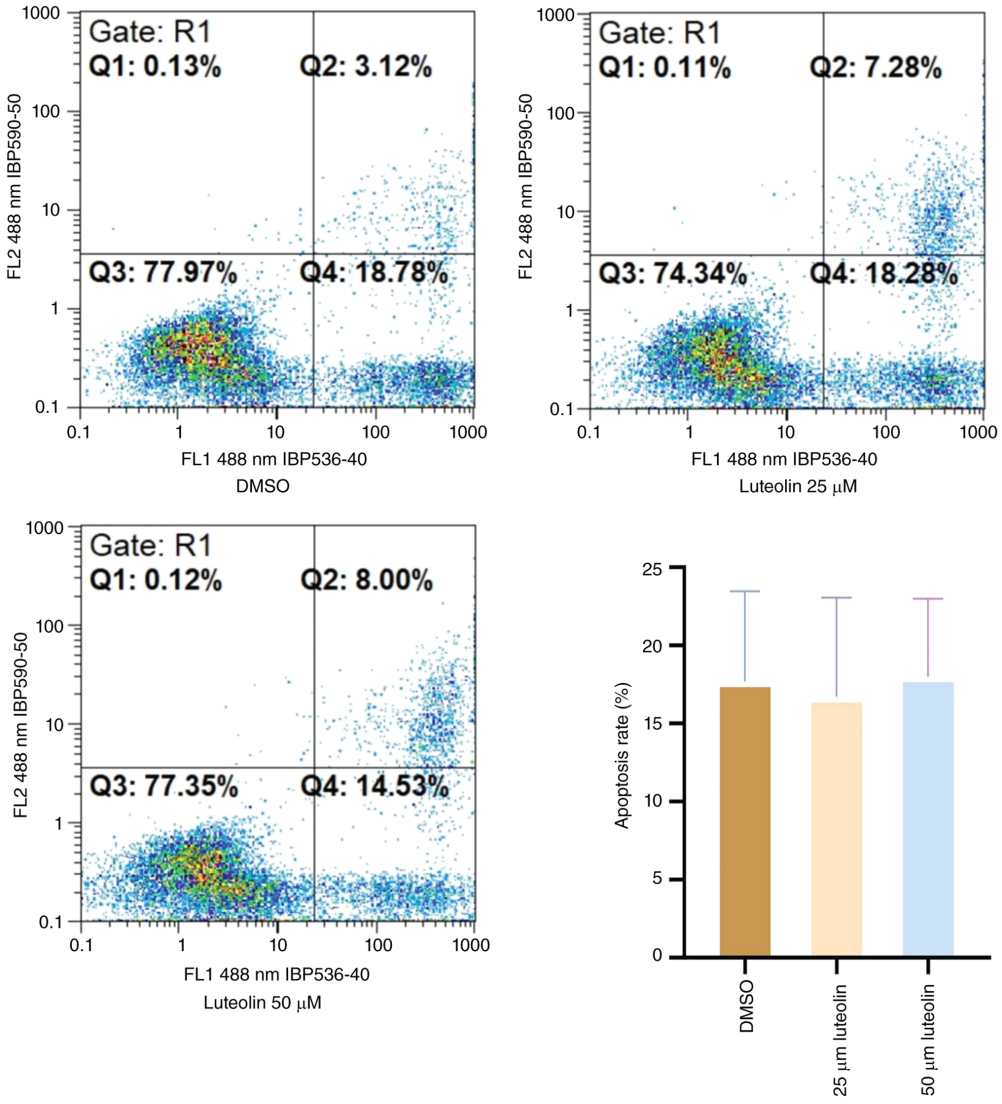

Figure 7. Effects of luteolin on the apoptosis of gastric cancer cells. Cells were treated with luteolin (25, 50 μM) for 48 h. Apoptosis was detected by flow cytometry. Values are expressed as the mean ± SD (n=3).

by suppressing tumor cell proliferation, inducing apoptosis, and regulating oncogene expression (16,17). Furthermore, the classical herbal formulation Erzhi Pill, composed of *Eclipta prostrata L.* and *Ligustrum lucidum*, has demonstrated improved efficacy in tumor therapy (18,19). Nevertheless, the specific active components and molecular mechanisms through which *Eclipta prostrata L.* exerts therapeutic effects against GC remain inadequately defined.

In the present study, the potential mechanisms underlying the anti-GC effects of *Eclipta prostrata L.* were investigated by combining network pharmacology with *in vitro* cellular experiments. The network pharmacology analysis identified several key bioactive compounds, including quercetin, luteolin and acacetin, which may regulate core targets such as AKT1, TNF, TP53, IL6, IL1B, CASP3, JUN, PTGS2, EGFR and HIF-1A. These targets are closely associated with critical biological processes involved in tumor progression, including cell proliferation, apoptosis and migration (12,20). Furthermore, MCODE clustering analysis indicated that Cluster 1 represents a major functional module within the interaction network.

Molecular docking analysis confirmed strong binding affinities between the identified compounds and the predicted core targets. Specifically, 3D structural conformations and 2D interaction profiling revealed that luteolin forms a stable network of conventional hydrogen bonds with all 10 core targets, indicating high target compatibility and favorable binding stability. Consistent with these structural observations, luteolin has been reported to show antitumor activity in various cancer models. For example, luteolin has been shown to inhibit prostate cancer cell proliferation by suppressing the AKT/mTOR signaling pathway (21). It can also reduce the proliferation and migration of esophageal cancer cells by regulating EMT (17). Similarly, luteolin has demonstrated synergistic effects when combined with chemotherapeutic agents or targeted therapies, helping to reverse drug resistance, enhance therapeutic efficacy, and reduce systemic toxicity (22,23). It has been reported that luteolin shows relatively low toxicity toward normal cells; concentrations effective against tumor cells produce minimal effects on normal gastric epithelial cells, and animal studies have shown no significant organ toxicity (24,25). Therefore, consistent with previous findings, luteolin may be the main

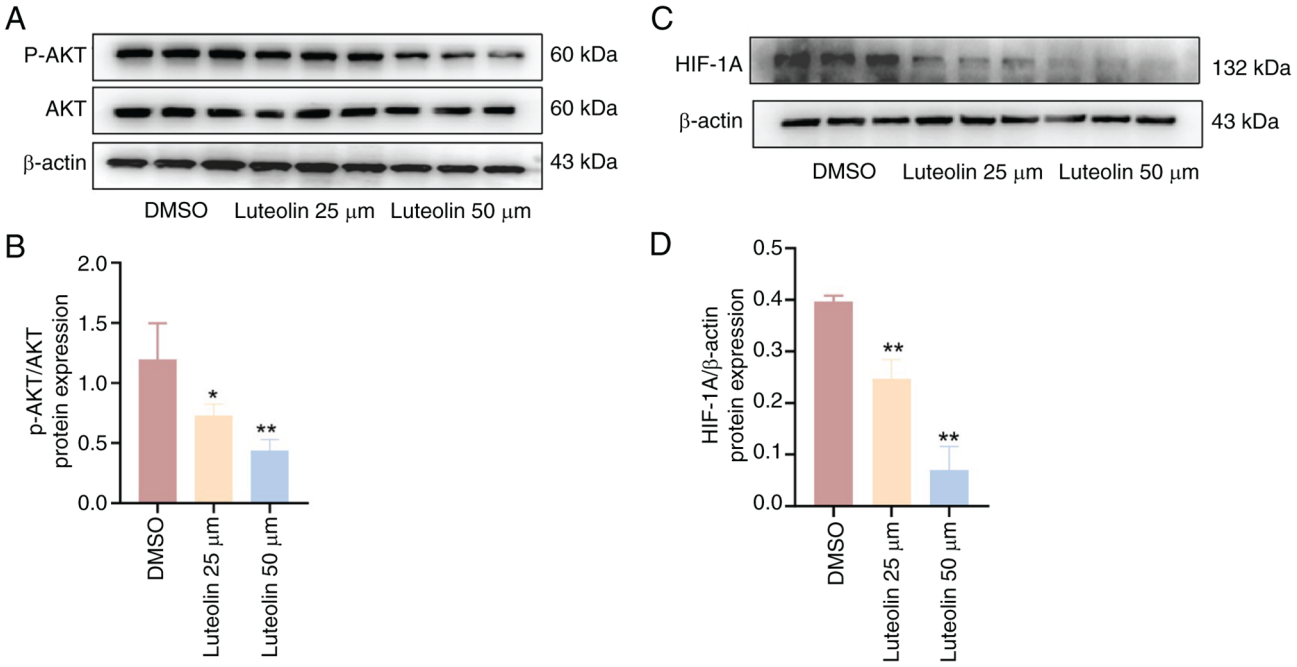

Figure 8. Effects of luteolin on the protein levels of phosphorylated AKT and HIF-1A in gastric cancer cells. (A) Western blot images showing the expression of P-AKT, total AKT, and β-actin in GC cells treated with DMSO (control), 25 μM luteolin, or 50 μM luteolin for 48 h. (B) Quantitative analysis of the relative protein expression of p-AKT/AKT. (C) Western blot images showing the expression of HIF-1A and β-actin under the same treatment conditions. (D) Quantitative analysis of the relative protein expression of HIF-1A/β-actin. Cells were treated with luteolin (25, 50 μM) for 48 h. Protein expression was detected by western blot analysis. Values are expressed as the mean ± SD (n=3). Compared with DMSO control, *P<0.05 and **P<0.01. AKT1, AKT serine/threonine kinase 1; HIF-1, hypoxia-inducible factor-1; p-, phosphorylated.

active component of *Eclipta prostrata L*. against GC. Luteolin formed hydrogen bonds with all 10 core targets and specifically bound to the key functional domains of GC-critical AKT1 and HIF-1A. Binding to AKT1's ATP-binding pocket may hinder its phosphorylation and activation, consistent with the present western blot results, which revealed reduced p-AKT levels. For HIF-1A, binding to its transactivation domain may impair its transcriptional activity, as supported by reduced *in vitro* HIF-1A expression (26). This aligns with reported luteolin regulatory mechanisms in gastric and other solid tumors, further confirming specific binding to functional domains as the key molecular basis for its anti-GC activity.

To further explore the potential bioactive components and therapeutic effects of *Eclipta prostrata L*. against GC, a CCK-8 assay was conducted to assess the effects of the key active compounds, quercetin, luteolin and acacetin, identified through network pharmacology analysis, on AGS cell proliferation. The results demonstrated that treatment with luteolin at appropriate concentrations significantly inhibited the proliferation and migration of AGS cells after 24-48 h of exposure, and its inhibitory effect was more pronounced than that of quercetin or acacetin. Of particular note, luteolin at concentrations that effectively inhibited the migration of GC cells displayed no cytotoxicity toward normal gastric mucosal epithelial GES-1 cells. This selective inhibitory effect suggests that luteolin can suppress the malignant migration of GC cells without damaging normal gastric mucosa, thus presenting favorable biosafety. Flow cytometric analysis revealed that treatment with luteolin (25 and 50 μM) for 48 h did not produce a statistically significant change in the apoptotic rate of AGS cells compared with the control group. These results suggest that luteolin, a major active constituent of *Eclipta prostrata L*., inhibits GC cells primarily by suppressing proliferation and migration rather than inducing apoptosis. Yang *et al* (17) isolated luteolin from *Eclipta prostrata L*. with a content of 0.21~0.35 mg/g dry weight and verified its potent anti-proliferative activity against cancer cells, which supports the selection of luteolin as the representative component for *in vitro* mechanistic verification in the present study.

KEGG pathway enrichment analysis identified several signaling pathways, including TNF signaling, PI3K-Akt signaling, p53 signaling and HIF-1 signaling, as potential mechanisms underlying the anti-GC effects of *Eclipta prostrata L*. The involvement of the PI3K-Akt pathway in regulating pathological processes has also been demonstrated in other disease models. For instance, studies on silica-induced pulmonary fibrosis have shown that Galectin-3 can regulate endothelial-to-mesenchymal transition through the PI3K/AKT signaling pathway, underscoring the conserved role of this pathway in controlling cellular phenotypic transitions and disease progression (27).

Extensive evidence indicates that aberrant activation of AKT1 contributes to tumor initiation and progression by regulating a range of cellular processes, including cell survival, proliferation, migration and metabolism (28-30). HIF-1A plays a critical role in tumor development. In the hypoxic tumor microenvironment, HIF-1A expression is significantly increased (31). As a key regulator of cellular adaptation to hypoxia, HIF-1A controls angiogenesis and metabolic reprogramming, particularly glucose metabolism, by regulating the transcription of numerous downstream target genes, promoting tumor progression (32,33). The present study confirmed

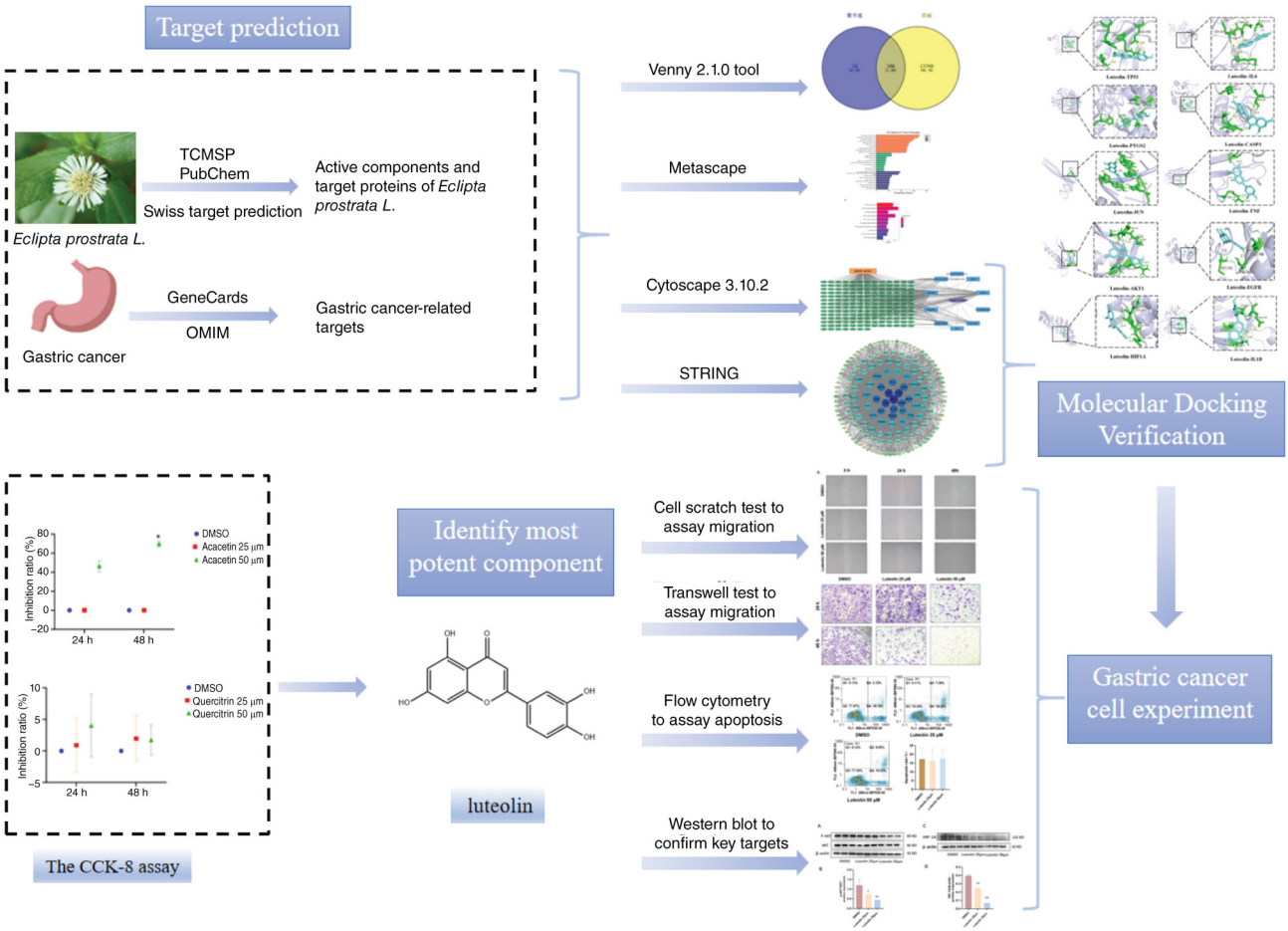

Figure 9. Schematic workflow showing the study process to explore *Eclipta prostrata L.'s* anti-gastric cancer mechanism, including target prediction, bioinformatic analyses, molecular docking, and cellular experiments focusing on the potent component luteolin. TCMSP, Traditional Chinese Medicine Systems Pharmacology Database and Analysis Platform; CCK-8, Cell Counting Kit-8.

that luteolin not only significantly inhibits the phosphorylation-dependent activation of AKT (the functionally active form of AKT1) but also significantly downregulates HIF-1A protein expression. These findings initially confirm that luteolin exerts a synergistic inhibitory effect on the occurrence and development of GC through dual regulation of AKT1 activity and the protein expression of HIF-1A, directly validating that these two core targets are key mediators of the anti-GC effect of *Eclipta prostrata L*. Notably, a previous study by the authors demonstrated that luteoloside (luteolin-7-O-glucoside), a key flavonoid glycoside from *Eclipta prostrata L*., exerted anti-GC effects via the p53/p21 signaling pathway (20). The present study further identified that luteolin, the aglycone of luteoloside, inhibits GC primarily through the AKT1/HIF-1A signaling pathway. These results indicate that different flavonoid components of *Eclipta prostrata L*. can suppress GC through distinct molecular mechanisms and signaling pathways. Building on the aforementioned analysis of cell-intrinsic signaling pathways, it is important to note that beyond cell-intrinsic signaling, tumors actively manipulate systemic homeostasis through neuroendocrine and metabolic pathways, creating a permissive environment for progression (34,35). Future studies should examine whether *Eclipta prostrata L*. or its components influence these systemic axes, potentially amplifying their therapeutic impact.

The present study integrated network pharmacology with *in vitro* experimental validation to explore the pharmacological basis and potential mechanisms underlying the anti-GC activity of *Eclipta prostrata L*. Network pharmacology analysis identified quercetin, luteolin and acacetin as the main active constituents. These compounds were predicted to interact with several key molecular targets, including AKT1, TNF and TP53, suggesting that the therapeutic effects of *Eclipta prostrata L*. may be achieved through the coordinated regulation of multiple targets and signaling pathways. As the major representative active component of *Eclipta prostrata L*. with the strongest anti-GC activity in the current screening, luteolin is a key material basis for the herb's antitumor effects, and its regulatory role in cancer-related signaling pathways is consistent with the anti-GC mechanisms of *Eclipta prostrata L*. extracts reported in existing literature. *In vitro* experiments further demonstrated that luteolin significantly inhibited the proliferation and migration of GC cells, reduced AKT1 phosphorylation, and decreased the protein expression level of HIF-1A. These findings provide direct experimental evidence supporting the identification of the key active component and molecular targets through which *Eclipta prostrata* L. exerts its therapeutic effects (Fig. 9). Several limitations in the present study should be noted. It is acknowledged that GeneCards and OMIM are comprehensive but not GC-specific databases that

may include some unvalidated cancer-related genes; however, multiple screening strategies were applied to minimize this bias. In addition, only the purified component, luteolin, was investigated, without evaluating the synergistic antitumor effects of multiple components in the herb. Furthermore, no *in vivo* animal models or GC cell lines of different molecular subtypes were included. Future studies will explore the synergistic effects of key herbal components, validate efficacy and safety in *in vivo* models and diverse GC cell lines, and investigate crude extracts to clarify further the anti-GC activity and mechanism of *Eclipta prostrata L*.

Acknowledgements

Not applicable.

Funding

The present study was supported by High-End Foreign Experts Project (grant no. G2022014132L) and Jiangsu Higher Education Institution Innovative Research Team For Science and Technology (2023) and Jiangsu Medical College Scientific and Technological Innovation Team (2024) and Medical Research General Program of Jiangsu Provincial Health Commission (grant no. M2024063) and Yancheng Science and Technology Basic Research Program (grants nos. YCBK202219 and YCBK2024046) and College-local collaborative innovation research project of Jiangsu Medical college (grant nos. 20239401, 202490403 and 202490408).

Availability of data and materials

The data generated in this study are included in the figures and/or tables of this article.

Authors' contributions

WY made substantial contributions to the conception and design of the study, and acquisition of funding, and participated in drafting the manuscript and revising it critically for important intellectual content. YC and FQ participated in research design and revised the manuscript. YC also conducted experiments, and contributed to the drafting, writing and revision of the manuscript. WX, XS and JW conducted experiments. XN performed data analysis and interpretation of data. YC and JW confirmed the authenticity of all the raw data. All authors read and approved the final version of the manuscript.

Ethics approval and consent to participate

Not applicable.

Patient consent for publication

Not applicable.

Competing interests

The authors declare that they have no competing interests.

References

1. Smyth EC, Nilsson M, Grabsch HI, van Grieken NC and Lordick F: Gastric cancer. Lancet 396: 635-648, 2020.
2. Agnarelli A, Vella V, Samuels M, Papanastasopoulos P and Giamas G: Incorporating immunotherapy in the management of gastric cancer: Molecular and Clinical Implications. Cancers (Basel) 14: 4378, 2022.
3. He Y, Zheng J, Ye B, Dai Y and Nie K: Chemotherapy-induced gastrointestinal toxicity: Pathogenesis and current management. Biochem Pharmacol 216: 115787, 2023.
4. Joshi SS and Badgwell BD: Current treatment and recent progress in gastric cancer. CA Cancer J Clin 71: 264-279, 2021.
5. Morgos DT, Stefani C, Miricescu D, Greabu M, Stanciu S, Nica S, Stanescu-Spinu II, Balan DG, Balcangiu-Stroescu AE, Coculescu EC, *et al*: Targeting PI3K/AKT/mTOR and MAPK signaling pathways in gastric cancer. Int J Mol Sci 25: 1848, 2024.
6. Gu Y, Sun M, Fang H, Shao F, Lin C, Liu H, Li H, He H, Li R, Wang J, *et al*: Impact of clonal TP53 mutations with loss of heterozygosity on adjuvant chemotherapy and immunotherapy in gastric cancer. Br J Cancer 131: 1320-1327, 2024.
7. Ding J, Gao W, Yang H, Duan L, Sun D, Liu L, Qu X, Yu H, Xu B, Zhao S, *et al*: KBTBD2 promotes proliferation and migration of gastric cancer via activating the EGFR signaling pathway. Pathol Res Pract 254: 155095, 2024.
8. Riquelme I, Pérez-Moreno P, Mora-Lagos B, Ili C, Brebi P and Roa JC: Long non-coding RNAs (lncRNAs) as regulators of the PI3K/AKT/mTOR pathway in gastric carcinoma. Int J Mol Sci 24: 6294, 2023.
9. Lu C, Ke L, Li J, Wu S, Feng L, Wang Y, Mentis AFA, Xu P, Zhao X and Yang K: Chinese medicine as an adjunctive treatment for gastric cancer: Methodological investigation of meta-analyses and evidence Map. Front Pharmacol 12: 797753, 2022.
10. Xie Z, Jiang N, Lin M, He X, Li B, Dong Y, Chen S and Lv G: The mechanisms of polysaccharides from tonic chinese herbal medicine on the enhancement of immune function: A review. Molecules 28: 7355, 2023.
11. Zhang X, Zhang C, Ren Z, Zhang F, Xu J, Zhang X and Zheng H: Curcumin affects gastric cancer cell migration, invasion and cytoskeletal remodeling through Gli1-β-catenin. Cancer Manag Res 12: 3795-3806, 2020.
12. Li X, Zhao L, Wang J, Ma T, Zhou J, Bian Y and Guo J: The Mechanism of Sijunzi decoction suppresses gastric cancer metastasis via the m6A methyltransferase METTL14 based on untargeted metabolomics studies and network pharmacology analysis. Drug Des Devel Ther 19: 2369-2392, 2025.
13. Timalsina D and Devkota HP: Eclipta prostrata (L.) L. (Asteraceae): Ethnomedicinal uses, chemical constituents, and biological activities. Biomolecules 11: 1738, 2021.
14. Qin T, Zhao J, Liu X, Li L, Zhang X, Shi X, Ke Y, Liu W, Huo J, Dong Y, *et al*: luteolin combined with low-dose paclitaxel synergistically inhibits epithelial-mesenchymal transition and induces cell apoptosis on esophageal carcinoma in vitro and in vivo. Phytother Res 35: 6228-6240, 2021.
15. Wang R, Li X, Xu Y, Li Y, Zhang W, Guo R and Song J: Progress, pharmacokinetics and future perspectives of luteolin modulating signaling pathways to exert anticancer effects: A review. Medicine (Baltimore) 103: e39398, 2024.
16. Zou YX, Mu ZQ, Wang J, Tian S, Li Y and Liu Y: Wedelolactone, a Component from Eclipta prostrata (L.) L., inhibits the proliferation and migration of head and neck squamous cancer cells through the AhR pathway. Curr Pharm Biotechnol 23: 1883-1892, 2022.
17. Yang J, Kim JS, Kwon YS, Seong ES and Kim MJ: Antioxidant and antiproliferative activities of eclipta prostrata (L.) L. Extract and isolated compounds. Molecules 28: 7354, 2023.
18. Fang Z, Xue Y, Leng Y, Zhang L, Ren X, Yang N, Chen J, Chen L and Wang H: Erzhi pills reverse PD-L1-mediated immunosuppression in melanoma microenvironment. Heliyon 10: e24988, 2024.
19. Qi Y, Li P, Li B, Lv P, Hu H, Tan C, Wang W, Jiang Y and He J: Integrating of serum pharmacochemistry, metabolomics, and experimental validation to explore the mechanism of Erzhi Pill against Triple-negative breast cancer. J Ethnopharmacol 353(Pt A): 120287, 2025.
20. Lin XX, Yang PQ, Li XJ, Xu ZZ, Wu HT, Hu SM, Yang XL, Ding Y and Yu WZ: Network pharmacology-based analysis and in vitro experimental verification of the inhibitory role of luteoloside on gastric cancer cells via the p53/p21 pathway. Oncol Lett 29: 76, 2024.
21. Li H, Wang X, Lu A, Pan Y, Zhang W and Hao L: Luteoloside inhibiting the prostate cancer cells growth and promoting the tumor cells autophagy through the AKT/mTOR pathway. J Men's Health 19: 49-55, 2023.

22. Dukel M and Zarzour F: luteolin enhances anticancer effects of PX-478 during hypoxic response in metastatic breast cancer cells. Anticancer Agents Med Chem 25: 1-10, 2025.
23. Ye S, Pan X, Zou L, Ni S, Zhang L, Hong Y and Hu K: HepG2 exosomes coated luteolin nanoparticles remodeling hepatic stellate cells and combination with sorafenib for the treatment of hepatocellular carcinoma. Cancer Nano 15: 15, 2024.
24. Ganai SA, Sheikh FA, Baba ZA, Mir MA, Mantoo MA and Yatoo MA: Anticancer activity of the plant flavonoid luteolin against preclinical models of various cancers and insights on different signalling mechanisms modulated. Phytother Res 35: 3509-3532, 2021.
25. Çetinkaya M and Baran Y: Therapeutic potential of luteolin on cancer. Vaccines (Basel) 11: 554, 2023.
26. Zhao Y, Xing C, Deng Y, Ye C and Peng H: HIF-1α signaling: Essential roles in tumorigenesis and implications in targeted therapies. Genes Dis 11: 234-251, 2023.
27. Cheng D, Lian W, Jia X, Wang T, Sun W, Liu Y and Ni C: LGALS3 regulates endothelial-to-mesenchymal transition via PI3K/AKT signaling pathway in silica-induced pulmonary fibrosis. Int J Mol Sci 509: 153962, 2024.
28. Degan SE and Gelman IH: Emerging roles for akt isoform preference in cancer progression pathways. Mol Cancer Res 19: 1251-1257, 2021.
29. Zhu Y, Yang J, Li Y, Xu J and Fang Z: Demethylase FTO enhances the PI3K/Akt signaling to promote gastric cancer malignancy. Med Oncol 40: 130, 2023.
30. Miricescu D, Totan A, Stanescu-Spinu II, Badoiu SC, Stefani C and Greabu M: PI3K/AKT/mTOR signaling pathway in breast cancer: From molecular landscape to clinical aspects. Int J Mol Sci 22: 173, 2020.
31. Shi S, Ou X, Liu C, Wen H and Ke J: Research progress of HIF-1a on immunotherapy outcomes in immune vascular microenvironment. Front Immunol 16: 1549276, 2025.
32. Rashid M, Zadeh LR, Baradaran B, Molavi O, Ghesmati Z, Sabzichi M and Ramezani F: Up-down regulation of HIF-1α in cancer progression. Gene 798: 145796, 2021.
33. Jin X, Dai L, Ma Y, Wang J and Liu Z: Implications of HIF-1α in the tumorigenesis and progression of pancreatic cancer. Cancer Cell Int 20: 273, 2020.
34. Wang YF, Dong ZK and Jin WL: Hijacking homeostasis: The brain-body neural circuitry in tumor pathogenesis and emerging therapeutic frontiers. Mol Cancer 24: 206, 2025.
35. Francis N and Borniger JC: Cancer as a homeostatic challenge: The role of the hypothalamus. Trends Neurosci 44: 903-914, 2021.